

Experimental and computational analysis of ribbing structure modification effect in tube and fin cross-flow heat exchangers operating at non-uniform inflow of media

Tomasz Bury, Małgorzata Hanuszkiewicz-Drapała*

Institute of Thermal Technology, Silesian University of Technology, ul. Konarskiego 22, 44-100 Gliwice, Poland

Abstract

Distributions of media streams flowing in a cross-flow tube and fin heat exchanger are usually non-uniform. This could be an effect of the heat exchanger construction, its installation method, design of a flowing channel or all those factors combined. The problem of the non-uniform media flow in heat exchangers of different types is not new, and it has been investigated by many researchers. Early results were sometimes ambiguous. More recent outcomes indicate that the effect of the non-uniform inflow of heat carriers to the heat exchanger could be significant—it may adversely affect the device's efficiency to a large extent. Investigations of tube and fin cross-flow heat exchangers carried out for almost twenty years at the Institute of Thermal Technology of the Silesian University of Technology, by way of experiments and numerical simulations, also confirm these latest conclusions. The reduction in overall heat exchanger capacity, comparing to the uniform inflow of media, may reach up to 18%. This work presents results of experimental and computational investigations of tube, fin, cross-flow, double row heat exchangers air-water. The heat exchangers under consideration are built in the form of two rows of elliptic tubes with rectangular fins. The ribbing structure of the first heat exchanger is uniform. This device was investigated primarily in order to determine its efficiency but also the range and the form of non-uniform inflow of air. The air flow distribution was tested on a special test station during a series of measurements. The results of the analysis of this heat exchanger were used to design a second heat exchanger with a non-uniform structure of fins on individual tubes. It was assumed that by changing the heat transfer surface (thickening the fins) in the region of high air speed, the efficiency of modified heat exchangers could be enhanced. Testing this hypothesis is the main aim of this work. The experimental results generally confirm the hypothesis, showing a rise in efficiency of up to 8%. However, it should be noted that the design of the modified ribbing structure is not optimal and changing this structure impacts the hydraulic resistance and distribution of air mass flow rate at the heat exchanger inflow. This effect should be considered when evaluating the results.

Keywords: Tube and fin cross-flow heat exchanger; non-uniform media inflow

1. Introduction

Studies carried out in recent years on finned tubular heat exchangers show that flow maldistribution adversely impacts heat exchanger performance [1, 2, 3]. In many cases investigations into heat exchangers have been numerical in character [2, 3]. Problems of flow maldistribution in heat exchangers have been analyzed previously. The results of investigations presented in [4, 5, 6, 7] claim that the effects of the flow maldistribution are minor or unimportant. Typically, numerical computational techniques are now used to perform thermal analyses of heat exchangers. Numerical models of cross-flow heat exchangers are presented among

others in [8, 9], and in [10, 11, 12] computational fluid dynamics (CFD) was applied in the analysis of heat exchangers.

The authors of [13, 14, 15] presented the results of experimental validation of a heat exchanger numerical model and the results of numerical analysis. Experimental and computational investigations of tube and fin cross-flow heat exchangers operating at non-uniform inflow of media have been carried out in the Institute of Thermal Technology of the Silesian University of Technology for a number of years [16, 17, 18]. The ANSYS Fluent program was used for computations for defined repetitive segments of the analyzed heat exchanger [18]. The finite difference method was implemented in the computer program [16] used for calculations relating to: tube and fin, cross-flow heat exchangers. The abovementioned numerical models were validated using experimental results and they were used for analyses of

*Corresponding author

Email address: malgorzata.hanuszkiewicz-drapala@polsl.pl
(Małgorzata Hanuszkiewicz-Drapała)

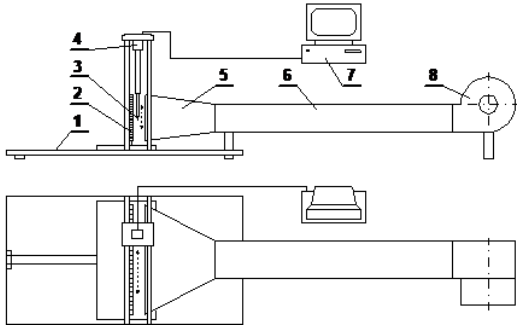


Figure 1: The air supply module (1—support plate, 2—heat exchanger, 3—thermo-anemometric sensor, 4—measuring probe, 5—diffuser, 6—channel, 7—control computer, 8—fan)

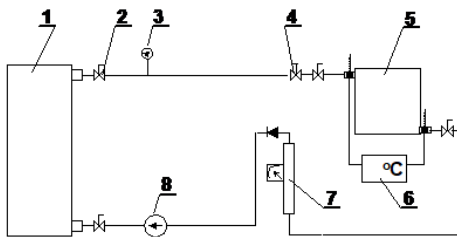


Figure 2: The hot water supply module (1—electric heater, 2—cut-out valve, 3—manometer, 4—control valve, 5—heat exchanger, 6—temperature measuring system, 7—flow meter, 8—pump)

typical single row tubes and fin, cross-flow heat exchangers with non-uniform media inflow.

This paper presents results of analyses of two types double row heat exchangers. Standard heat exchanger is built in the form of a double row of elliptic tubes with rectangular fins in a uniform ribbing structure. In the case of the modified heat exchanger, the ribbing structure is non-uniform. Numerical analyses presented in this paper were produced using a computer code based on the finite difference method [16].

2. Test station

The test station was designed as part of the project [16] in order to determine the form and scope of a non-uniform inflow of air to a cross-flow heat exchanger. The original part of this test station—the air supply module—is shown in Fig. 1. The main element of the test station is a thermo-anemometric sensor where the shifting is controlled by a computer. It enables the air temperature and velocity to be measured at the heat exchanger inlet and outlet.

The original configuration of the test station only allowed for “cold” measurements to be taken. Broader based experiments became possible after the test station was upgraded by adding a hot water supply module—see Fig. 2.

Three parameters are assumed as independent and may be set by the researcher: the air and water volumetric flow rates and the water inlet temperature.

3. Experimental and computational analysis

3.1. Measuring procedure

The air temperature and velocity distribution measurements are predicated on defining the measuring task in the form of an input file for the program controlling the measuring probe work. The main part of that file contains information about the measuring grid. A regular measuring grid was used for the measurements. The grid divides the whole measuring cross section into identical rectangles, with the measuring nodes located in the middle. The air inlet and outlet velocity distributions are measured by the V1T type thermo-anemometric sensor in 140 points located on the inlet or outlet plane. The dimensions of the sensor shifting area are a little smaller than those of the air inflow area. This is due to the risk of the sensor being damaged by colliding with the inlet diffuser walls.

The time constant of the measurement and the number of measurements performed in each node should be entered in the input file. The time constant was 0.5 s. During this time, the sampling of velocity and temperature takes place with the maximum frequency allowed by the measuring system (50 MHz). The measurement in each point is repeated 30 times. The results are analyzed on-line (identification of random errors, type A uncertainty calculation). The air velocity and temperature values with their uncertainties at each measuring point are recorded on the computer hard disk.

The measuring program was started after steady state conditions were achieved. The time needed to achieve steady state operation of the test station ranges between 15 and 25 minutes depending on the set of independent parameters. The hot water parameters (temperature and volumetric flow rate) are recorded every 15 s during the experiment. Those data sets are also analyzed in order to obtain the final result and its uncertainty.

3.2. Data analysis methodology

The total heat flow rates for the heat exchanger are obtained from the experiments. This parameter could be calculated as the increase in air enthalpy:

$$\dot{Q}_a = \dot{V}_a \rho_a c_p a (t_{a\ out} - t_{a\ in}) \quad (1)$$

where \dot{V}_a is the air volumetric flow rate, ρ_a is the air density, c_p is the air specific heat capacity at constant pressure, and $t_{a\ in}$, $t_{a\ out}$ are the air inlet and outlet temperatures, respectively. These temperatures are calculated as the surface area-weighted average values for the inlet and outlet planes. However, there is a problem involved here: the volumetric air flow rate is determined at the end of the rectangular flow channel and there are some air leaks upstream of the heat exchanger (mostly through the measuring probe shifting hole). For this reason, it is better to calculate the total heat transfer rate as the water enthalpy drop:

$$\dot{Q}_w = \dot{V}_w \rho_w c_w (t_{w\ in} - t_{w\ out}) \quad (2)$$

where \dot{V}_w is the water volumetric flow rate, ρ_w is the water density, c_w is the specific heat capacity, and t_{win} , t_{wout} are the water inlet and outlet temperatures, respectively. The density of water has been assumed according to thermodynamic tables for the outlet temperature.

3.3. Measurements of the standard heat exchanger

The core of the standard heat exchanger (marked as HE-3) is built by two rows of elliptic tubes (ten in each row) with plate, rectangular fins. The heat exchanger view is shown in Fig. 3. The device is made of steel. The basic dimensions of the tube and fin are given in Fig. 4. The tube wall thickness is 1 mm and the tube length is 490 mm. The spacing of fins in the first row is 6.0 mm (81 fins on each tube) and in the second row 3.5 mm (140 fins on each tube). Selected results of experiments made for the HE-3 unit are presented in Table 1.

3.4. Computational analysis

3.4.1. Numerical model of the heat exchanger [16]

The mathematical model of the considered heat exchanger was created taking into account simplifying assumptions [16]. The most important assumptions are as follows:

- steady state conditions,
- one-dimensional agents flow,
- no internal heat sources,
- radiation is neglected,
- heat losses are neglected,
- heat flow is normal to a boundary,
- real fin is replaced with a round or a plate-elliptic fin of the same surface.

It was assumed that the air inflow is non-uniform and the water inflow may be non-uniform. The influence of temperature on thermal properties of the heat carriers was taken into account. The analyzed real cross-flow heat exchanger was replaced with a model rectangular heat exchanger. The model was then divided into elementary fragments (Fig. 5). Each fragment represents a recurrent element of the real heat exchanger—a single tube with the fin.

The energy balance equations for each fragment constitute the mathematical basis of the model [16]. Assuming that the water flows along the X axis and the air flows along the Y axis the energy balance for a recurrent fragment may be written as follows:

$$\begin{aligned} d\dot{Q} &= -\dot{m}_w c_{pw} \frac{\partial T_w}{\partial x} dx = \dot{m}_a c_{pa} \frac{\partial T_a}{\partial y} dy \\ &= \alpha_a (T_m - T_a) dA \end{aligned} \quad (3)$$

where \dot{m} is the mass flow rate, α_a is an average heat transfer coefficient at the gas side for all the ribbed surface and T_m is the average temperature of rib and pipe surface.

As the inlet temperatures of the media are known, the following boundary conditions may be used:

$$T_w(0, y, z) = T_{w,in} \quad T_a(x, 0, z) = T_{a,in} \quad (4)$$

The mass flow rates of the agents are described by the following formulas:

$$d\dot{m}_w = \frac{g_w \cdot \dot{m}_w}{Y_{\max} Z_{\max}} dy dz \quad (5)$$

$$d\dot{m}_a = \frac{g_a \cdot \dot{m}_a}{X_{\max} Z_{\max}} dx dz \quad (6)$$

The inequality factors g_w and g_a are defined as below:

$$g_w = \frac{w_w}{w_{w,m}} \quad (7)$$

$$g_a = \frac{w_a}{w_{a,m}} \quad (8)$$

The subscript “m” in Equations 7 and 8 means the average velocity of the medium. Information about the non-uniform flow of the air is put into the model on the basis of measurements. A non-uniform water inlet to the exchanger may be set arbitrarily by a function or on the basis of numerical simulations [16].

The control volume method based model of heat transfer for the recurrent fragment of the heat exchanger was created to calculate the average temperature of the ribs and tube outer surface. A detailed description of the model and equations can be found in [16].

The parameters calculated using the model of the recurrent fragment are: outlet and average temperature of the water flowing in the pipe, average temperature of the air, average temperature of the rib and the pipe surface, average values of the heat transfer coefficients on the gas side and the heat flow rate transferred in the recurrent fragment. The heat transfer coefficient from the hot water to the pipe was computed from Colburn’s formula:

$$Nu = 0.023 \cdot Re^{0.8} \cdot Pr^{1/3} \quad (9)$$

The heat transfer coefficient on the gas side may be determined by way of the numerical simulations for a numerical model of the recurrent fragment of the considered heat exchanger [19] or may be computed from one of the available Nusselt number correlations.

The calculation procedure for the whole exchanger model is iterative and it is repeated for all the recurrent fragments of the considered heat exchanger. First, the air temperature increase in the analyzed fragment is assumed. Next, the heat transfer coefficients for the water and the air are calculated as well as the rib and pipe surface average temperature. The heat flow rate transferred in the recurrent fragment is then computed and the accuracy criterion is checked. If the criterion is satisfied, the procedure is realized for the next fragment. If the criterion is not fulfilled, the described procedure is then repeated for the given recurrent fragment until the required accuracy is achieved.

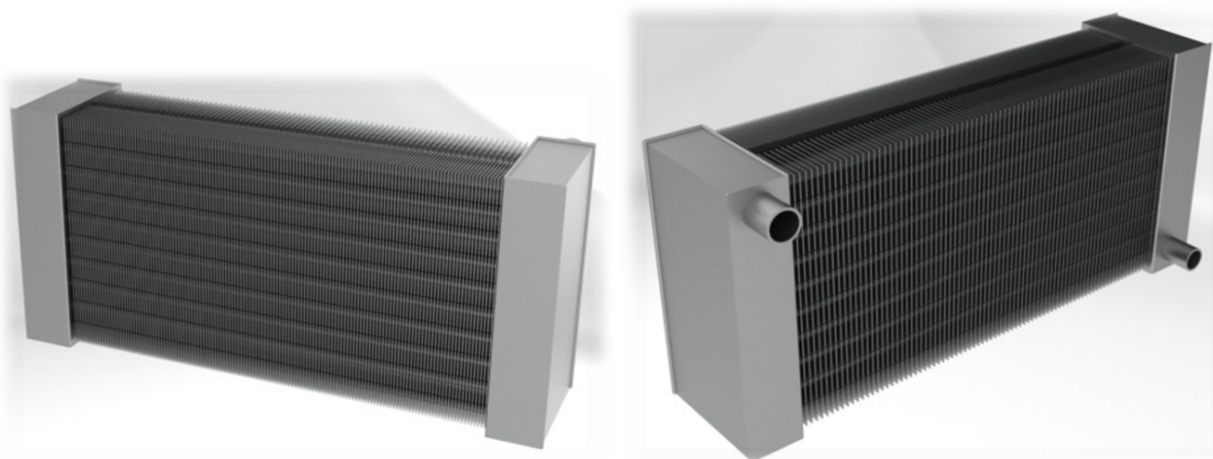


Figure 3: View of the HE-3 heat exchanger

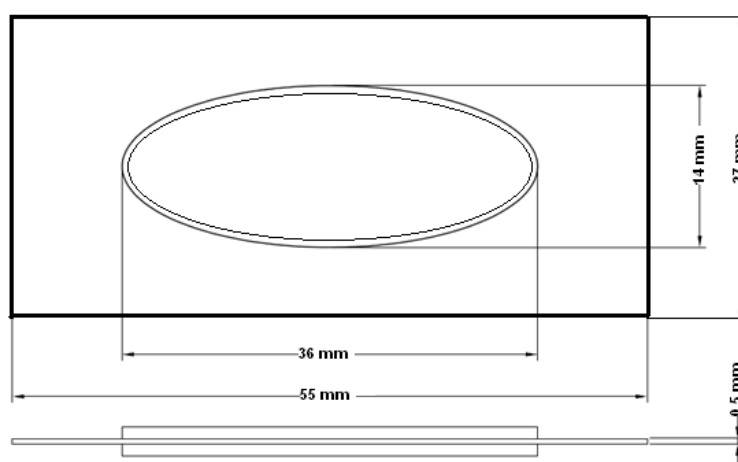


Figure 4: Basic dimensions of tubes and fins

Table 1: Selected experimental results for the HE-3 heat exchanger

Measurement identification code	Air volumetric flow rate, m ³ /h	Boiler outlet temperature setpoint, °C	Water volumetric flow rate, dm ³ /min	Water inlet temperature, °C	Water outlet temperature, °C	Heat flow rate, kW
HE3-1	6450	50	28.8	49.8	45.4	8.75
HE3-2		60	28.7	59.9	53.8	12.05
HE3-3		70	28.6	69.2	61.4	15.30
HE3-4		80	28.3	80.1	70.5	18.54
HE3-5		90	28.1	88.5	77.1	21.79
HE3-6	5100	50	28.3	50.4	46.4	7.81
HE3-7		60	28.1	59.8	54.1	11.02
HE3-8		70	27.9	70.4	62.8	14.53
HE3-9		80	27.6	80.2	70.7	17.90
HE3-10		90	27.3	89.7	78.3	21.15
HE3-11	4250	50	28.3	51.1	47.2	7.62
HE3-12		60	27.7	60.1	54.7	10.29
HE3-13		70	27.8	71.2	64.3	13.13
HE3-14		80	27.3	80.1	71.9	15.27
HE3-15		90	27.5	89.9	80.5	17.55

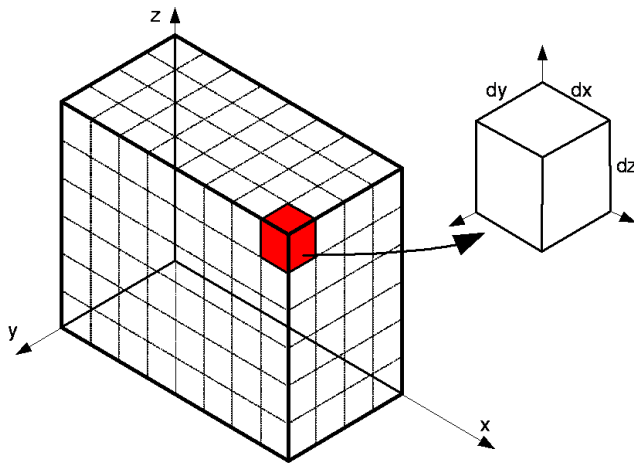


Figure 5: The model heat exchanger and the recurrent fragment

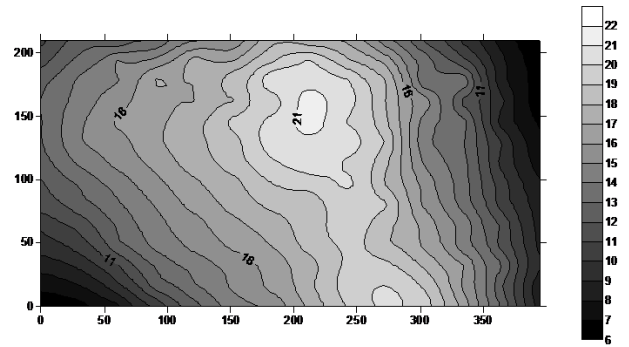


Figure 7: Sample inlet air velocity distribution (m/s) for the maximum fan capacity

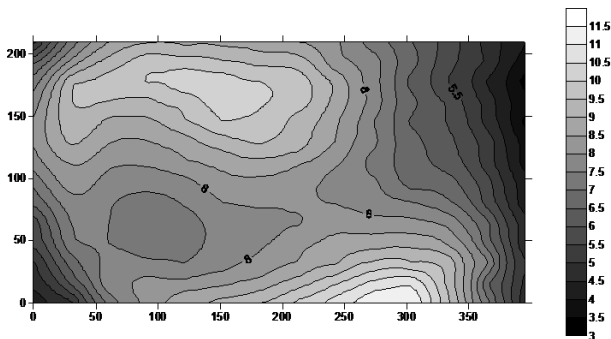


Figure 6: Sample inlet air velocity distribution (m/s) for the minimum fan capacity

Table 2: Structure of the proposed heat exchanger

Pipe No. (from top to bottom)	HE-3M	
	1 st row	2 nd row
1	FE60	FE70
2	FE70	FE70
3	FE70	FE70
4	FE280	FE70
5	FE280	FE70
6	FE280	FE70
7	FE70	FE70
8	FE70	FE70
9	FE60	FE70
10	FE60	FE70

FE280—pipe length 490 mm, 175 plate ribs every 2.8 mm
 FE60—pipe length 490 mm, 81 plate ribs every 6.0 mm
 FE70—pipe length 490 mm, 140 plate ribs every 3.5 mm

ing the results the fins structure as shown in Table 2 were proposed for the considered heat exchangers.

3.4.2. Modified heat exchanger design

The review of the current state of knowledge presented in the introductory section shows that media flow maldistribution could significantly impact heat exchanger performance. An obvious hypothesis assumes that making the media flow more uniform increases the total heat flow rates transferred in the heat exchanger. This hypothesis has been partially confirmed by experiments [20], as well as the hypothesis assuming that modelling of the air flow can also lead to some improvement [18].

The proposed heat exchanger with special fins structure presented in this paper can improve the capacity of this device. The general idea of this hypothesis is that extending the heat transfer surface in the region where gas flow is more intensive would also intensify heat transport.

The fins structure could only be designed properly if the gas flow structure is known (velocity distribution at the exchanger inlet). In the analyzed cases, it was assumed that the basis for the modified heat exchanger (HE-3m) design are the air inlet velocity distributions obtained for the standard heat exchanger. Sample air velocity distributions measured for the HE-3 heat exchanger are presented in Figs. 6 and 7. Some variations in the air non-uniformity form were observed, depending on the fan capacity, but after averag-

3.4.3. Results of numerical simulations

Two series of numerical simulations were carried out. Assessment of the non-uniform inflow of media to the standard heat exchanger HE-3 was the aim of the first series. The results are shown in Table 3. The performance of the modified heat exchanger HE-3m was simulated in the second series. Relative differences of the numerically predicted heat transfer rates and measured heat transfer rates were calculated according to the formula:

Table 3: Results of numerical simulations

Case codification code	HE-3		HE-3m	
	Q, kW	δ , %	Q, kW	δ , %
1	10.03	14.6	9.59	9.6
2	13.79	14.5	13.19	9.5
3	17.52	14.5	16.75	9.5
4	21.36	15.2	20.44	10.2
5	25.32	16.2	24.23	11.2
6	8.89	13.8	8.50	8.8
7	12.50	13.4	11.95	8.4
8	16.45	13.2	15.72	8.2
9	20.47	14.4	19.58	9.4
10	24.47	15.7	23.41	10.7
11	8.64	13.5	8.26	8.5
12	11.69	13.6	11.17	8.6
13	14.95	13.8	14.29	8.8
14	17.42	14.1	16.66	9.1
15	20.11	14.6	19.23	9.6

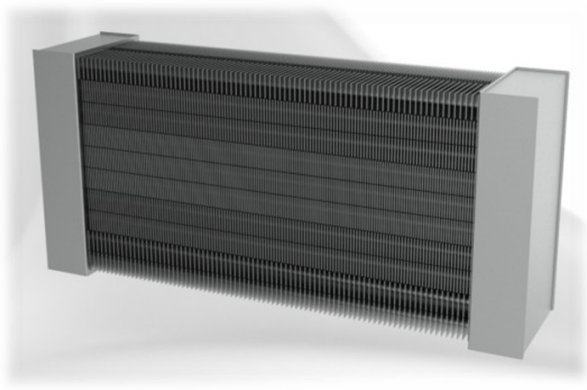


Figure 8: Front view of the modified HE-3m heat exchanger

$$\delta = \frac{\dot{Q}_{num} - \dot{Q}_{ex}}{\dot{Q}_{ex}} 100\% \quad (10)$$

The experimental heat flow rates \dot{Q}_{ex} were taken for the HE-3 unit (last column in Table 1). Numerical values \dot{Q}_{num} for the HE-3 heat exchanger were calculated, assuming that the total air flow rate spreads equally over the whole heat exchanger inlet. When calculating the total heat transfer rates for the modified HE-3m heat exchanger, it was assumed that the air inlet velocity distribution is the same as measured for the HE-3 unit at a given total air inflow rate. The case identification code refers to the measurement number given in Table 1.

The results presented in Table 3 indicate that non-uniform inflow of air and water may reduce the capacity of the considered heat exchanger by up to 16%. The predicted increase in heat exchanger capacity resulting from the special fins structure (last column of Table 3) seems quite promising. The average value is about 10% and that render this approach worthy of consideration.

3.5. Modified heat exchanger measurements

Fig. 8 presents the view of the front side of the HE-3m unit. The heat exchanger was made by the GEA Heat Exchangers Company according to the specification given in section 3.4.2. Measurements done for the HE-3m unit were analyzed according to the methodology described in section 3.2. The results are gathered in Table 4.

3.6. Comparative analysis

The heat transfer rates computed as the water enthalpy drop for both analyzed devices were then compared and the relative differences between were calculated. Selected outcomes of this analysis are set out in Table 5.

The results of experiments for the HE-3M heat exchanger show some enhancement of its performance compared to the HE-3 unit. The increase in the total heat transfer rates reaches 9.2% and this could be seen as a significant effect. When evaluating these results it is important to take into account the uncertainties of the measurements. The special

fins structure was designed for higher air flow rates, as can be seen in the last column of Table 5. The case ID refers to the measurement number given in Tables 1 and 4. It can be seen that the recorded relative differences are generally smaller than predicted by the numerical simulations. However, for cases 1 to 5, the increase in heat exchanger capacity is close to 10%.

4. Conclusions

It has been numerically and experimentally confirmed that the hypothesis which assumes that a specially designed heat exchanger whose fins structure fits certain media flow conditions may perform better than a standard one. Experimental data confirm the hypothesis only for high air flow rates. The results obtained for low air inflow are somewhat inconclusive—some increase in the heat exchanger capacity was observed, but the level of increment is within the bounds of measurements uncertainties. The most important reason why this situation arises is the fact that the distribution of the air velocity inflowing to the modified units is different than the one taken into account when designing the special fins structure. This is due to a change of hydraulic resistance in the flow. Moreover, the fins structure of the HE-3m unit was optimized for the upper range of the air flow rates.

The computationally predicted effects of the special fins structure application are slightly more optimistic, which is caused by using the air inflow data taken from the standard HE-3 unit measurements.

In light of all above mentioned facts the following conclusion may be withdrawn: a heat exchanger with a specially designed fins structure could provide a positive solution in cases where a media flow maldistribution cannot be mitigated (subject to a commercial evaluation of course). The design procedure of the fins structure should be optimized for certain media flow rates. It is difficult to find a satisfying solution when the media flow varies across an appreciable range, as in the case at hand.

Acknowledgments

This work was sponsored by the Ministry of Science and Higher Education under Statutory Research Funds of the Faculty of Energy and Environmental Engineering, Silesian University of Technology (Poland).

References

- [1] X. Luo, W. Roetzel, U. Lüdersen, The single-blow transient testing technique considering longitudinal core conduction and fluid dispersion, *International Journal of Heat and Mass Transfer* 44 (1) (2001) 121–129.
- [2] N. Srihari, S. K. Das, Transient response of multi-pass plate heat exchangers considering the effect of flow maldistribution, *Chemical Engineering and Processing: Process Intensification* 47 (4) (2008) 695–707.
- [3] K. Shaji, S. K. Das, The effect of flow maldistribution on the evaluation of axial dispersion and thermal performance during the single-blow testing of plate heat exchangers, *International Journal of Heat and Mass Transfer* 53 (7) (2010) 1591–1602.

Table 4: Selected experimental results for the HE-3m heat exchanger

Measurement identification code	Air volumetric flow rate, m ³ /h	Boiler outlet temperature setpoint, °C	Water volumetric flow rate, dm ³ /min	Water inlet temperature, °C	Water outlet temperature, °C	Heat flow rate, kW
HE3m-1	6450	50	28.8	51.0	46.2	9.54
HE3m-2		60	28.8	59.3	52.7	13.09
HE3m-3		70	28.6	69.5	61.0	16.67
HE3m-4		80	28.5	79.3	68.9	20.25
HE3m-5		90	28.2	88.5	76.1	23.79
HE3m-6	5100	50	28.8	50.3	46.1	8.35
HE3m-7		60	28.9	61.1	55.2	11.73
HE3m-8		70	28.7	69.8	61.9	15.54
HE3m-9		80	28.4	79.6	69.9	18.81
HE3m-10		90	28.2	89.4	77.7	22.43
HE3m-11	4250	50	28.9	50.6	46.6	7.98
HE3m-12		60	28.7	60.3	54.9	10.66
HE3m-13		70	28.5	70.7	63.7	13.66
HE3m-14		80	28.4	80.3	72.2	15.69
HE3m-15		90	28.3	89.1	79.7	18.06

Table 5: Results of the comparative analysis

Case ID	HE-3			HE-3m			Relative difference HE-3m – HE-3, %
	Heat flow rate, kW	Standard uncertainty, kW	Standard uncertainty, %	Heat flow rate, kW	Standard uncertainty, kW	Standard uncertainty, %	
1	8.75	±0.33	±3.76	9.54	±0.33	±3.45	9.06
2	12.05	±0.27	±2.22	13.09	±0.27	±2.05	8.62
3	15.30	±0.27	±1.78	16.67	±0.27	±1.63	9.00
4	18.54	±0.40	±2.14	20.25	±0.28	±1.37	9.19
5	21.79	±0.27	±1.22	23.79	±0.27	±1.12	9.22
6	7.81	±0.49	±6.28	8.35	±0.31	±3.76	6.87
7	11.02	±0.26	±2.38	11.73	±0.26	±2.24	6.40
8	14.53	±0.30	±2.10	15.54	±0.30	±1.96	6.97
9	17.90	±0.27	±1.53	18.81	±0.27	±1.45	5.11
10	21.15	±0.41	±1.95	22.43	±0.27	±1.21	6.05
11	7.62	±0.57	±7.44	7.98	±0.33	±4.18	4.76
12	10.29	±0.33	±3.17	10.66	±0.33	±3.06	3.60
13	13.13	±0.29	±2.18	13.66	±0.29	±2.09	4.03
14	15.27	±0.40	±2.65	15.69	±0.27	±1.72	2.74
15	17.55	±0.39	±2.21	18.06	±0.26	±1.45	2.96

- [4] R. Berryman, C. Russell, The effect of maldistribution of air flow on aircooled heat exchanger performance, Maldistribution of flow and its effect on heat exchanger performance, JB Kitto, JM Robertson ASME Htd 75 (1987) 19–23.
- [5] C. Meyer, D. Kröger, Plenum chamber flow losses in forced draught air-cooled heat exchangers, Applied Thermal Engineering 18 (9) (1998) 875–893.
- [6] S. Nair, S. Verma, S. Dhingra, Rotary heat exchanger performance with axial heat dispersion, International Journal of Heat and Mass Transfer 41 (18) (1998) 2857–2864.
- [7] K.-S. Lee, S.-J. Oh, Optimal shape of the multi-passage branching system in a single-phase parallel-flow heat exchanger, International Journal of Refrigeration 27 (1) (2004) 82–88.
- [8] A. Korzeń, D. Taler, Modeling of transient response of a plate fin and tube heat exchanger, International Journal of Thermal Sciences 92 (2015) 188–198.
- [9] D. Taler, M. Trojan, J. M. Taler, Mathematical modeling of cross-flow tube heat exchangers with a complex flow arrangement, Heat Transfer Engineering 35 (14-15) (2014) 1334–1343.
- [10] B. Sundén, Computational fluid dynamics in research and design of heat exchangers, Heat Transfer Engineering 28 (11) (2007) 898–910.
- [11] M. M. A. Bhutta, N. Hayat, M. H. Bashir, A. R. Khan, K. N. Ahmad, S. Khan, Cfd applications in various heat exchangers design: A review, Applied Thermal Engineering 32 (2012) 1–12.
- [12] S. Jun, V. M. Puri, 3d milk-fouling model of plate heat exchangers using computational fluid dynamics, International journal of dairy technology 58 (4) (2005) 214–224.
- [13] E. Dario, L. Tadrist, J. Oliveira, J. Passos, Measuring maldistribution of two-phase flows in multi-parallel microchannels, Applied Thermal Engineering 91 (2015) 924–937.
- [14] Z. Zhang, S. Mehendale, J. Tian, Y. Li, Experimental investigation of distributor configuration on flow maldistribution in plate-fin heat exchangers, Applied Thermal Engineering 85 (2015) 111–123.
- [15] S. Datta, P. Das, S. Mukhopadhyay, Performance of a condenser of an automotive air conditioner with maldistribution of inlet air—simulation studies and its experimental validation, International Journal of Heat and Mass Transfer 98 (2016) 367–379.
- [16] R. Piątek, Analiza termodynamiczna ożebrowanego wymiennika ciepła z nierównomiernym dopływem czynników [Thermal analysis of a plate-and-fin tube heat exchanger with a non-uniform inflow of mediums], Ph.D. thesis, Institute of Thermal Technology, Silesian University of Technology, Poland (2003).
- [17] T. Bury, J. Składzień, M. Hanuszkiewicz-Drapała, Experimental and numerical analyses of a non-uniform agents flow impact on a finned cross-flow heat exchanger effectiveness, in: Proceedings of the 22nd International Conference on Efficiency, Cost, Optimization, Simulation and Environmental Impact of Energy Systems - ECOS 2009, Foz do Iguacu, Parana, Brazil, 2009.
- [18] K. Widziwicz, Analiza termodynamiczna krzyżowoprądowego wymiennika ciepła z uwzględnieniem nierównomierności dopływu czynników i promieniowania cieplnego [Thermodynamic analysis of a cross-flow heat exchanger including a non-uniform inflow of mediums and the radiative heat transfer], Ph.D. thesis, Institute of Thermal Technology, Silesian University of Technology, Poland (2014).
- [19] T. Bury, J. Składzień, The experimental and the numerical analysis of a ribbed heat exchanger with an unequal inlet of the air, Proceedings of Heat Transfer and Renewable Sources of Energy (2006) 419–426.
- [20] T. Bury, J. Składzień, Evaluation of selected methods of mitigation of media flow maldistribution impact in finned cross-flow heat exchangers., in: 3rd International Conference on Contemporary Problems of Thermal Engineering, Gliwice, 2012.